

Article

# Disclosing the Sensitivity and Selectivity of Metal Oxide/Graphene Oxide-Based Chemoresistors towards VOCs †

Eleonora Pargoletti <sup>1,2,\*</sup> , Antonio Tricoli <sup>3</sup> , Mariangela Longhi <sup>1,2</sup> , Gian Luca Chiarello <sup>1,2</sup>   
and Giuseppe Cappelletti <sup>1,2</sup> 

- <sup>1</sup> Dipartimento di Chimica, Università degli Studi di Milano, Via Golgi 19, 20133 Milan, Italy; mariangela.longhi@unimi.it (M.L.); gianluca.chiarelo@unimi.it (G.L.C.); giuseppe.cappelletti@unimi.it (G.C.)
- <sup>2</sup> Consorzio Interuniversitario Nazionale per la Scienza e Tecnologia dei Materiali (INSTM), Via Giusti 9, 50121 Firenze, Italy
- <sup>3</sup> Nanotechnology Research Laboratory, Faculty of Engineering, University of Sydney, Sydney, NSW 2006, Australia; antonio.tricoli@sydney.edu.au
- \* Correspondence: eleonora.pargoletti@unimi.it
- † Presented at the 8th International Symposium on Sensor Science, 17–26 May 2021; Available online: <https://i3s2021dresden.sciforum.net/>.

**Abstract:** Nowadays, gas sensors play a vital role in a plethora of applications. However, there are still some important shortcomings, such as the scarce selectivity and sensitivity, especially at low operating temperatures. Herein, we report the successful sensing achieved by tailoring the chemoresistive materials comprised of graphene oxide (GO) sheets well-integrated in a three-dimensional network of n-type metal oxide semiconductors (MOS). Thanks to the synergistic effect between GO and MOS under UV light, we obtained a very good sensitivity (down to 100 ppb) towards different volatile organic compounds (VOCs, i.e., ethanol, acetone, ethylbenzene, toluene) even at room temperature. Moreover, the best performing sensor (SnO<sub>2</sub>/GO 32:1) resulted in being highly selective towards polar compounds, such as acetone.



**Citation:** Pargoletti, E.; Tricoli, A.; Longhi, M.; Chiarello, G.L.; Cappelletti, G. Disclosing the Sensitivity and Selectivity of Metal Oxide/Graphene Oxide-Based Chemoresistors towards VOCs. *Eng. Proc.* **2021**, *6*, 18. <https://doi.org/10.3390/I3S2021Dresden-10163>

Published: 19 May 2021

**Publisher's Note:** MDPI stays neutral with regard to jurisdictional claims in published maps and institutional affiliations.



**Copyright:** © 2021 by the authors. Licensee MDPI, Basel, Switzerland. This article is an open access article distributed under the terms and conditions of the Creative Commons Attribution (CC BY) license (<https://creativecommons.org/licenses/by/4.0/>).

**Keywords:** gas sensors; metal oxide; graphene oxide; volatile organic compounds; sensitivity; selectivity; temperature; light

## 1. Introduction

The development of high-performing sensing materials, able to detect ppb-trace concentrations of Volatile Organic Compounds (VOCs) at low temperatures in the presence of interfering species, is mandatory for the development of next-generation miniaturized wireless sensors [1–3]. Herein, we present the engineering of highly sensitive chemical sensors, comprising of different Metal Oxide Semiconductors (MOS as WO<sub>3</sub>, ZnO, SnO<sub>2</sub> and a SnO<sub>2</sub>-TiO<sub>2</sub> solid solution) layouts coupled with Graphene Oxide (GO) material. These innovative 3D networks showed promising features in terms of both sensitivity (down to ppb level) and selectivity (towards a specific VOC).

## 2. Materials and Methods

### 2.1. N-Type Semiconductors Synthesis, Electrodes Preparation and Sensing Tests

Four different n-type semiconductors, namely WO<sub>3</sub>, ZnO, SnO<sub>2</sub>, and Sn<sub>0.55</sub>Ti<sub>0.45</sub>O<sub>2</sub> solid solution, were chosen to be grown onto graphene oxide (GO) material by following a very easy hydrothermal method already reported in our previous works [4–8]. According to earlier studies, we adopted 32:1 salt precursor-to-GO weight ratio, since it resulted in being the optimal one in terms of sensing performances at low operating temperatures.

Once synthesized, the as-prepared composites were deposited onto Pt-based interdigitated electrodes (IDEs) by hot-spray method, using 2.5 mg mL<sup>-1</sup> ethanol powders suspension and spraying 4 mL of it. The air-brush pressure (0.8 bar), the temperature of

the heating plate (230 °C), and the deposition height (8 cm) were kept constant. A final calcination step at 350 °C for 1 h was performed to guarantee good powder film adhesion on IDEs. Sensing measurements were performed, adopting the chamber already described elsewhere [7]. Four different VOCs, i.e., ethanol, acetone, ethylbenzene, and toluene, were investigated as the analyte species. The sensor response is reported as:  $(R_{\text{air}}/R_{\text{analyte}}) - 1$ , where  $R_{\text{air}}$  is the film resistance in air and  $R_{\text{analyte}}$  is the film resistance at a given concentration of the target gas. We also computed the sensor response ( $t_{\text{res}}$ , which is the time needed to reach 90% of the sensor response) and the recovery times ( $t_{\text{rec}}$ , which is the time necessary to recover 90% of the final response).

## 2.2. Powders Physico-Chemical Characterizations

Specific surface area and porosity distribution were determined by  $N_2$  adsorption/desorption isotherms at 77 K using a Micromeritics Tristar II 3020 (Norcross, GA, USA) apparatus and the instrumental software (Version 1.03) applying Brunauer–Emmett–Teller (BET) and Barrett–Joyner–Halenda analyses, respectively. Before measurements, sample powders were pretreated at  $T = 150$  °C (4 h under  $N_2$  flux) to remove adsorbed species.

X-ray Powder Diffraction (XRPD) analyses were performed on a Philips PW 3710 Bragg–Brentano goniometer equipped with a scintillation counter,  $1^\circ$  divergence slit, 0.2 mm receiving slit, and  $0.04^\circ$  Soller slit systems. We used graphite-monochromated Cu  $K_\alpha$  radiation (Cu  $K_{\alpha 1}$   $\lambda = 1.54056$  Å,  $K_{\alpha 2}$   $\lambda = 1.54433$  Å) at 40 kV  $\times$  40 mA nominal X-rays power. Diffraction patterns were collected between  $10^\circ$  and  $70^\circ$  with a step size of  $0.1^\circ$ . A microcrystalline Si-powder sample was employed as a reference to correct instrumental line broadening effects.

To evaluate powders optical band gaps ( $E_g$ ) by Kubelka–Munk elaboration, Diffuse Reflectance Spectra (DRS) were measured on a UV/Vis spectrophotometer Shimadzu UV-2600 spectrophotometer (Kyoto, Japan) equipped with an integrating sphere; a “total white”  $BaSO_4$  powder was used as reference.

## 3. Results and Discussion

Four different n-type semiconductors ( $WO_3$ , ZnO,  $SnO_2$ , and a solid solution of  $SnO_2$ - $TiO_2$ ) grown onto GO sheets were finely characterized on several physico-chemical points of view (see Table 1).

**Table 1.** Specific surface area ( $S_{\text{BET}}$ ), total pores volume ( $V_{\text{tot. pores}}$ ) by Brunauer–Emmett–Teller (BET) analysis, average crystallite domain size by X-ray powder diffraction ( $\langle d^{\text{XRPD}} \rangle$ ), and optical band gap ( $E_g$ ) of the investigated samples.

Sample	$S_{\text{BET}}$ ( $\text{m}^2 \text{g}^{-1}$ )	$V_{\text{tot. pores}}$ ( $\text{cm}^3 \text{g}^{-1}$ )	$\langle d^{\text{XRPD}} \rangle$ (nm)	$E_g$ (eV)
$WO_3$ /GO 32:1	6	0.014	50	2.71
ZnO/GO 32:1	11	0.050	40	3.07
$SnO_2$ /GO 32:1	55	0.133	8	3.40
$Sn_{0.55}Ti_{0.45}O_2$ /GO 32:1	117	0.119	7	3.20

Specifically, active surface area ( $S_{\text{BET}}$ ) together with total pores volume ( $V_{\text{tot. pores}}$ ), average domain size by X-ray diffraction analysis ( $\langle d^{\text{XRPD}} \rangle$ ), and optical band gap ( $E_g$ ) were determined to possibly give insights into the role played by these features in tailoring the final sensing response. Analyzing data reported in Figure 1a, it seems that  $SnO_2$  matrix can guarantee better performances at both high (350 °C) and low (25 °C, UV-assisted) operating temperatures, resulting in greater sensor intensity at 1 ppm of acetone concentration, with respect to the other investigated materials. As already finely explained in our previous work, this may be ascribable to the grain boundary density of the different MOS-GO nanoheterojunctions. Indeed, the change in material resistance depends mainly on the ratio between the grain size ( $d$ ) and the Debye length ( $\delta$ ). If  $d$  is slightly lower or equal to  $2\delta$ , the whole grains are depleted and change in the surface oxygen species concentration can influence the entire grain, resulting in higher sensitivity. Here, the

particle sizes of SnO<sub>2</sub>-GO (~5–8 nm) are very close to twice the Debye length of tin dioxide (~3 nm). Therefore, an improvement of the sensing behavior is justified. Notably, the Sn<sub>0.55</sub>Ti<sub>0.45</sub>O<sub>2</sub>/GO 32:1 solid solution did not show any observable response at room temperature (RT), but the lowest reachable value was 250 °C. All the tested materials were able to sense 100 ppb of acetone even at RT conditions, by exploiting the UV light thanks to the synergistic effect between n-type MOS and p-type GO [4,8]. Indeed, when the device is irradiated by UV light, the photo-excited electron-hole couples can split up. In particular, some holes can desorb the adsorbed oxygen ions on the MOS surface, forming O<sub>2</sub> gaseous molecules and provoking a depletion layer reduction and a free carrier concentration increase. Moreover, the higher carrier density can concomitantly cause more atmospheric oxygen molecules to adsorb onto the MOS surface, therefore creating photo-induced oxygen ions that are weakly bound and can react more easily with the VOC molecules. When the reaction occurs, electrons are released back to the conduction band of the metal oxide, decreasing the surface depletion layer and rising the final conductivity up.

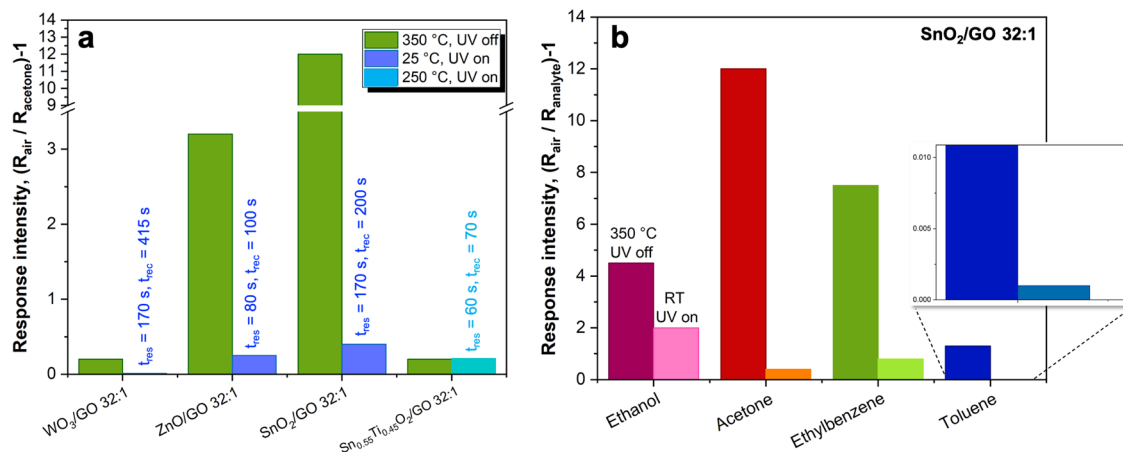


**Figure 1.** (a) Sensors response intensities towards 1 ppm of acetone at both 350 °C (without UV light aid) and 25 °C or 250 °C (only for Sn<sub>0.55</sub>Ti<sub>0.45</sub>O<sub>2</sub>/GO 32:1) UV-assisted. Inset: average response and recovery times computed on responses relative to different acetone concentrations (for tests carried out at 25 °C). (b) Selectivity comparison obtained with the highest performing sample, SnO<sub>2</sub>/GO 32:1, towards several VOCs (1 ppm) at both 350 °C (UV off) and 25 °C (UV on).

Instead, as far as it concerns the response and recovery times at RT (inset of Figure 1a), ZnO/GO 32:1 revealed to be the most promising one exhibiting the fastest behavior (around 90 s for both parameters).

Since the tin dioxide-based sensor was believed to be the optimal one, it was further tested towards different VOC species, such as ethanol, ethylbenzene, and toluene. Figure 1b displays a comparison of the sensor signal intensity at 1 ppm, both at 350 °C (without the UV light) and 25 °C (UV light-aided). It seems that, at higher temperatures, SnO<sub>2</sub>/GO 32:1 compound can selectively sense acetone, whereas by decreasing the operating conditions, a higher polar molecule such as ethanol could be detected more easily. This is probably due to the different VOCs chemical structures, such as the presence of polar groups (hydroxyl groups) or steric hindrance, thus leading to their different affinity with the MOS surface. It has already been reported that alcohols show higher sensing responses than aldehydes or ketones and, to a greater extent, non-polar/low polar analytes, such as benzene-derivatives.

#### 4. Conclusions

In this work, we finely investigated the sensing performances of different 3D nano-networks of n-type semiconductors coupled with graphene oxide materials. We highlighted that, by tailoring the MOS, it is possible to tune the final sensitivity and selectivity, reaching very promising results even at room temperature by exploiting the UV light. Particularly, the synergistic effect between n-type MOS and p-type GO plays a pivotal role in boosting

the chemoresistors features. Hence, we believe that the present study can pave the way for the engineering of optimal sensing low-temperature devices to be used as diagnostic tools.

**Supplementary Materials:** The following are available online at <https://www.mdpi.com/article/10.3390/I3S2021Dresden-10163/s1>.

**Author Contributions:** Conceptualization, E.P., A.T. and G.C.; methodology, E.P., A.T., G.L.C. and G.C.; validation, E.P.; formal analysis, E.P. and M.L.; investigation, E.P.; data curation, E.P.; writing—original draft preparation, E.P.; writing—review and editing, A.T., M.L., G.L.C. and G.C.; supervision, G.C.; funding acquisition, G.C. All authors have read and agreed to the published version of the manuscript.

**Funding:** This work received financial support from the Università degli Studi di Milano through the “PSR2019 Azione A” project.

**Institutional Review Board Statement:** Not applicable.

**Informed Consent Statement:** Not applicable.

**Data Availability Statement:** Data is contained within the article.

**Acknowledgments:** In this section, you can acknowledge any support given which is not covered by the author contribution or funding sections. This may include administrative and technical support, or donations in kind (e.g., materials used for experiments).

**Conflicts of Interest:** The authors declare no conflict of interest.

## References

1. Fusco, Z.; Rahmani, M.; Bo, R.; Verre, R.; Motta, N.; Käll, M.; Neshev, D.; Tricoli, A. Nanostructured Dielectric Fractals on Resonant Plasmonic Metasurfaces for Selective and Sensitive Optical Sensing of Volatile Compounds. *Adv. Mater.* **2018**, *30*, e1800931. [[CrossRef](#)] [[PubMed](#)]
2. Pineau, N.J.; Kompalla, J.F.; Güntner, A.T.; Pratsinis, S.E. Orthogonal gas sensor arrays by chemoresistive material design. *Microchim. Acta* **2018**, *185*, 563. [[CrossRef](#)] [[PubMed](#)]
3. Güntner, A.T.; Abegg, S.; Königstein, K.; Gerber, P.A.; Schmidt-Trucksäss, A.; Pratsinis, S.E. Breath Sensors for Health Monitoring. *ACS Sens.* **2019**, *4*, 268–280. [[CrossRef](#)] [[PubMed](#)]
4. Pargoletti, E.; Hossain, U.H.; Di Bernardo, I.; Chen, H.; Tran-Phu, T.; Lipton-Duffin, J.; Cappelletti, G.; Tricoli, A. Room-temperature photodetectors and VOC sensors based on graphene oxide-ZnO nano-heterojunctions. *Nanoscale* **2019**, *11*, 22932–22945. [[CrossRef](#)] [[PubMed](#)]
5. Pargoletti, E.; Tricoli, A.; Pifferi, V.; Orsini, S.; Longhi, M.; Guglielmi, V.; Cerrato, G.; Falciola, L.; Derudi, M.; Cappelletti, G. An electrochemical outlook upon the gaseous ethanol sensing by graphene oxide-SnO<sub>2</sub> hybrid materials. *Appl. Surf. Sci.* **2019**, *483*, 1081–1089. [[CrossRef](#)]
6. Americo, S.; Pargoletti, E.; Soave, R.; Cargnoni, F.; Trioni, M.I.; Chiarello, G.L.; Cerrato, G.; Cappelletti, G. Unveiling the acetone sensing mechanism by WO<sub>3</sub> chemiresistors through a joint theory-experiment approach. *Electrochim. Acta* **2021**, *371*, 137611. [[CrossRef](#)]
7. Pargoletti, E.; Verga, S.; Chiarello, G.L.; Longhi, M.; Cerrato, G.; Giordana, A.; Cappelletti, G. Exploring Sn<sub>x</sub>Ti<sub>1-x</sub>O<sub>2</sub> Solid Solutions Grown onto Graphene Oxide (GO) as Selective Toluene Gas Sensors. *Nanomaterials* **2020**, *10*, 761. [[CrossRef](#)] [[PubMed](#)]
8. Pargoletti, E.; Hossain, U.H.; Di Bernardo, I.; Chen, H.; Tran-Phu, T.; Chiarello, G.L.; Lipton-Duffin, J.; Pifferi, V.; Tricoli, A.; Cappelletti, G. Engineering of SnO<sub>2</sub>-Graphene Oxide Nanoheterojunctions for Selective Room-Temperature Chemical Sensing and Optoelectronic Devices. *ACS Appl. Mater. Interfaces* **2020**, *12*, 39549–39560. [[CrossRef](#)] [[PubMed](#)]